Alexandria Engineering Journal (2013) **52**, 507–516

Alexandria University

Alexandria Engineering Journal

www.elsevier.com/locate/aej
www.sciencedirect.com

ORIGINAL ARTICLE

Artificial neural network and response surface methodology modeling in mass transfer parameters predictions during osmotic dehydration of *Carica papaya* L.

J. Prakash Maran [a,*], V. Sivakumar [a], K. Thirugnanasambandham [a], R. Sridhar [b]

[a] *Department of Food Technology, Kongu Engineering College, Perundurai, Erode 638 052, TN, India*
[b] *Tamil Nadu Pollution Control Board, Salem 635 004, TN, India*

Received 12 January 2013; revised 17 April 2013; accepted 20 June 2013
Available online 9 July 2013

KEYWORDS

Artificial neural network;
Response surface methodology;
Papaya;
Mass transfer;
Osmotic dehydration

Abstract In this study, a comparative approach was made between artificial neural network (ANN) and response surface methodology (RSM) to predict the mass transfer parameters of osmotic dehydration of papaya. The effects of process variables such as temperature, osmotic solution concentration and agitation speed on water loss, weight reduction, and solid gain during osmotic dehydration were investigated using a three-level three-factor Box-Behnken experimental design. Same design was utilized to train a feed-forward multilayered perceptron (MLP) ANN with back-propagation algorithm. The predictive capabilities of the two methodologies were compared in terms of root mean square error (RMSE), mean absolute error (MAE), standard error of prediction (SEP), model predictive error (MPE), chi square statistic (χ^2), and coefficient of determination (R^2) based on the validation data set. The results showed that properly trained ANN model is found to be more accurate in prediction as compared to RSM model.

* Corresponding author. Tel.: +91 4294 226606; fax: +91 4294 220087.
E-mail addresses: prakashmaran@gmail.com (J. Prakash Maran), drvsivakumar@yahoo.com (V. Sivakumar), thirusambath5@gmail.com (K. Thirugnanasambandham), sridhar36k@yahoo.co.in (R. Sridhar).

Peer review under responsibility of Faculty of Engineering, Alexandria University.

ELSEVIER Production and hosting by Elsevier

1. Introduction

India is the second largest producer of fruits and vegetables contributing about 12.4% to the total world fruit and 13.3% to vegetable production. India ranks first in the production of mangoes (41%), banana (28%), papaya (30%), and peas (30%) and second in brinjal (29%), cauliflower (29%), onion (18%), and cabbage (8%). Papaya (*Carica papaya* L.) is rich in carbohydrate, vitamin A, calcium, iron, and fiber and has negligible saturated fat. Apart from this, it contains niacin,

1110-0168 © 2013 Production and hosting by Elsevier B.V. on behalf of Faculty of Engineering, Alexandria University.
http://dx.doi.org/10.1016/j.aej.2013.06.007

foliate, vitamin E, magnesium, phosphorus, potassium, lipids, and amino acids. Papaya is the only natural source of papain – an effective natural digestive aid – which breaks down protein and cleanses of the digestive track. Papaya is highly seasonal fruit and only available during the month of March to June in India, and it is mostly cultivated in the states of Andhra Pradesh, Karnataka, Gujarat, Orissa, West Bengal, Assam, Tamil Nadu, Kerala, Madhya Pradesh, and Maharashtra. Since it is a perishable commodity, papaya becomes much cheaper in terms of selling price during the peak season and also it leads to more financial losses to the grower resulting from the spoilage of fruits in larger quantities. Preservation of these fruits can prevent a huge wastage and make them available in the off-season at remunerative prices [1].

Removal of water from solid food is a form of food preservation, inhibiting the growth of microorganisms, besides preventing a large part of biochemical reactions that occur due to the presence of moisture [2]. Among various methods used for extending the shelf life of fruit such as Papaya (*Carica papaya* L.), osmotic dehydration is one of the simplest and inexpensive processes that are not only energy-saving and also low-capital investment. Osmotic dehydration is used as a pre-treatment to many preservation processes such as freezing, freeze-drying, microwave drying, and air-drying to improve nutritional, sensorial, and functional properties of fruits without changing their integrity [3]. Osmotic dehydration is widely used for the partial removal of water from plant tissues by immersion in a hypertonic (osmotic) solution. The driving force for the diffusion of water from the tissue into the solution is provided by the higher osmotic pressure of the hypertonic solution. During osmotic dehydration, water removal from the product is always accompanied by the simultaneous counter diffusion of solutes from the osmotic solution into the tissue [4]. The osmotic solution used must have a low water activity (a_w), and moreover, the solute must be harmless with good taste. The type of osmotic agent used for osmotic dehydration is a very important factor that determines the rate of diffusion and quality of the final product. Jaggery is concentrated sugar cane juice containing 75–85% sucrose, which is widely used as a substitute of white and refined cane sugar in India. Jaggery is used as ayurvedic/traditional medicines for treating throat and lung infections and also used for the preparation of sweet confectionery items [5]. Among the various osmotic agents used in the literature, jaggery is found to be more suitable because of its medicinal characteristics and its nutritional value [6]. The number of publications has been reported in the literature to know the influence of variables such as temperature, concentration of the osmotic solution, the size and geometry of the material, the solution to material mass ratio, and the level of agitation of the solution on mass transfer rates for different products using different osmotic solutions. [7–12].

The response surface methodology (RSM) has been widely and effectively used method in process and product improvement. It is widely used to examine and optimize the operational variables for experiment designing, model developing, etc., [13,14]. RSM is typically used for mapping a response surface over a particular region of interest, optimizing the responses, or for selecting operating conditions to achieve target specifications or consumer requirements [15]. Several studies on the optimized conditions for the osmotic dehydration process using RSM have been published for papaya, potato, diced pepper, and banana [16–18].

Artificial neural network (ANN) is a powerful modeling technique that offers several advantages over conventional modeling techniques because they can model based on no assumptions concerning the nature of the phenomenological mechanisms and understanding the mathematical background of problem underlying the process and the ability to learn linear and nonlinear relationships between variables directly from a set of examples. Artificial neural networks have already been applied to simulate processes such as fermentation [19], cross-flow microfiltration [20], drying behavior of different food and agricultural materials such as carrot [15,21], tomato [22], ginseng [23], cassava, mango [24], and osmotic dehydration [25]. Hence, the main motivation behind the study is to develop an approach for the evaluation of mass transfer during osmotic dehydration process by using RSM and ANN techniques.

In this study, a response surface methodology and artificial network model (ANN) models were developed to predict the mass transfer during osmotic dehydration of papaya. A number of experiments were carried out based on Box-Behnken experimental design to collect the output variables such as water loss (WL), weight reduction (WR), and solid gain (SG) as a function of osmotic temperature (30, 40, and 50 °C), osmotic solution concentration (40, 50, and 60 °brix), and agitation speed (100, 150, and 200 rpm). An effective RSM model and a feed-forward neural network on back-propagation were developed utilizing the experimental data, and the efficiency of both models was compared.

2. Materials and methods

2.1. Raw materials

Papaya (with similar maturity and weight) was used as raw materials in the experiments and was purchased from a local market near Erode, Tamil Nadu. Samples were stored at 4 °C prior to the experiments. Osmotic solution was prepared by mixing of appropriate amount of jaggery with the proper amount of water.

2.2. Experimental procedure

For each experiment, the papaya was washed, peeled manually, and cut into 1 cm × 1 cm × 1 cm cubes. The papaya cubes were washed in water to remove the fines adhering to the surface of the cubes. The desired concentration of osmotic solution of jaggery was prepared and the known weight of papaya cubes was immersed in the Erlenmeyer flasks which contain osmotic solutions of different concentrations (40, 50, and 60 °brix) at different temperatures (30, 40, and 50 °C) and agitation speeds (100, 150, and 200 rpm). Osmotic dehydration was carried out in a temperature and agitation controlled incubator shaker (GeNei, model SLM-INC-OS-16, India). To prevent evaporation from the osmotic solution, Erlenmeyer flaks were covered with a plastic wrap during the experiments. During the osmotic treatment, every half-an-hour the cubes were removed from osmotic solution and weighed after removing the solution adhering to the surface using filter paper (Whatman No 1), and this procedure was continued until the weight of the samples remained constant. Experiments were randomized in order to minimize the effects of unexplained variability in the observed responses due to extraneous factors. All the experiments were performed in triplicate, and the average value was used for the determination of water loss, solid gain, and weight reduction.

2.3. Mathematical calculations

During osmotic dehydration process, the water loss and solid gain take place simultaneously. The weight of the papaya was reduced due to water loss, but at the same time, there will be an increase in the weight due to solid gain. The mass exchange between the solution and samples was evaluated by using the parameters such as water loss (WL), solid gain (SG), and weight reduction (WR), and those parameters were calculated by the following equations [26]

$$\mathrm{WR}(\%) = \frac{W_0 - W_t}{W_0} \times 100 \quad (1)$$

$$SG(\%) = \frac{S_t - S_0}{W_0} \times 100 \quad (2)$$

$$\mathrm{WL}(\%) = \mathrm{WR} + \mathrm{SG} \quad (3)$$

where W_0 is the initial weight of papaya cubes (g), W_t the weight of papaya cubes after osmotic dehydration for any time t (g), S_0 is the initial dry weight of papaya (g), and S_t is dry weight of papaya after osmotic dehydration for time t (g).

2.4. Response surface methodology modeling

Response surface methodology is an empirical statistical modeling technique employed for multiple regression analysis using quantitative data obtained from properly designed experiments to solve multivariate equations simultaneously [27]. A Box-Behnken Design (BBD) with three factors at three levels was used to design the experiments and it is exhibited in Table 2. The process parameters (independent variables) selected for the optimization were osmotic temperature (X_1), osmotic solution concentration (X_2), and agitation speed (X_3). The number of experiments (N) required for the development of BBD is defined as $N = 2\,k(k-1) + C_o$ (where k is number of factors and C_o is the number of central point). The design included 17 experiments with 5 central points. Each independent variable was coded at three levels between +1, 0, and −1, whereas osmotic temperature: 30–50 °C; osmotic solution concentration: 40–60 °brix, and agitation speed: 100–200 rpm, respectively. Coding of the variables was done according to the following equation:

$$x_i = \frac{x_i - x_{cp}}{\Delta x_i} \quad i = 1,\ 2,\ 3\ \ldots\ k \quad (4)$$

where x_i, dimensionless value of an independent variable; X_i, real value of an independent variable; X_{cp}, real value of an independent variable at the center point; and ΔX_i, step change in real value of the variable i corresponding to a variation in a unit for the dimensionless value of the variable i.

Performance of the process was evaluated by analyzing the responses (Y), which depend on the input factors x_1, $x_2\ldots$, x_k, and the relationship between the response and the input process parameters is described by

$$Y = f(x_1,\ x_2 \ldots x_k) + e \quad (5)$$

where f is the real response function the format of which is unknown and e is the error which describes the differentiation.

A second-order polynomial equation was used to fit the experimental data to identify the relevant model terms using statistical software (Design Expert 8.0.7.1). A quadratic model, which also includes the linear model, can be described as:

$$Y = \beta_0 + \sum_{j=1}^{k} \beta_j x_j + \sum_{j=1}^{k} \beta_{jj} x_j^2 + \sum_{i} \sum_{<j=2}^{k} \beta_{ij} x_i x_j + e_i \quad (6)$$

where Y is the response; x_i and x_j are variables (i and j range from 1 to k); β_0 is the model intercept coefficient; β_j, β_{jj}, and β_{ij} are interaction coefficients of linear, quadratic, and the second-order terms, respectively; k is the number of independent parameters (k = 4 in this study); and e_i is the error [28].

The statistical analysis was performed using Design Expert Statistical Software package 8.0.7.1 (Stat Ease Inc., Minneapolis, USA). The experimental data were analyzed using multiple regressions, and the significance of regression coefficients was evaluated by F-test. Modeling was started with a quadratic model including linear, squared, and interaction terms, and the model adequacies were checked in terms of the values of R^2, adjusted R^2, and prediction error sum of squares (PRESS). The significant terms in the model were found by Pareto analysis of variance (ANOVA) for each response, and ANOVA

Table 1 Error functions and its equations.

Error function	Equation and number	Ref.
Root mean square error	$\mathrm{RMSE} = \sqrt{\sum_{i=1}^{n} (Y_i, e - Y_{i,p})^2 / n}$ (10)	[34]
Mean absolute error	$\mathrm{MAE} = \frac{i}{n} \sum_{i=1}^{n} \lvert Y_i, e - Y_{i,p} \rvert$ (11)	[35]
Standard error of prediction (%)	$\mathrm{SEP}(\%) = \frac{RMSE}{Y}_{i,e} \times 100$ (12)	[34]
Model predictive error (%)	$\mathrm{MPE}(\%) = \frac{100}{n} \sum_{i=1}^{n} \left\lvert \frac{Y_{i,e} - Y_{i,p}}{Y_{i,p}} \right\rvert$ (13)	[36]
Chi square statistic (χ^2)	$\chi^2 = \sum_{i=1}^{n} \frac{(Y_{i,p} - Y_{i,e})^2}{Y_{i,p}}$ (14)	[37]
Correlation coefficient (R^2)	$R^2 = \frac{\sum_{i=1}^{n} (Y_{i,p} - Y_{i,e})}{\sum_{i=1}^{n} (Y_{i,p} - Y_e)^2}$ (15)	[38]

n is the number of experiments; $Y_{i,e}$ is the experimental value of the ith experiment; $Y_{i,e}$ is the predicted value of the ith experiment by model; and Y_e is the average value of experimentally determined values.

Table 2 Coded and un-coded Box-Behnken design of independent variables and their corresponding experimental and predicted values.

Run	X_1 (°C)	X_2 (°brix)	X_3 (rpm)	Water loss (%)			Weight reduction (%)			Solid gain (%)		
				Y_{EXP}	Y_{RSM}	Y_{ANN}	Y_{EXP}	Y_{RSM}	Y_{ANN}	Y_{EXP}	Y_{RSM}	Y_{ANN}
1	30 (−1)	40 (−1)	150 (0)	45.24	46.38	45.32	34.26	35.35	34.43	13.26	13.24	13.28
2	40 (0)	60 (1)	100 (−1)	63.76	63.71	63.18	61.56	61.95	61.79	10.36	10.48	10.37
3	40 (0)	50 (0)	150 (0)	53.51	53.51	53.51	50.47	50.47	50.78	12.56	12.56	12.63
4	40 (0)	60 (1)	200 (1)	72.01	72.59	71.46	65.38	65.22	65.59	16.37	16.02	16.26
5	30 (−1)	60 (1)	150 (0)	69.12	69.74	68.73	62.79	63.66	62.64	12.83	13.05	12.57
6	40 (0)	50 (0)	150 (0)	53.51	53.51	53.51	50.47	50.47	50.78	12.56	12.56	12.63
7	50 (1)	40 (−1)	150 (0)	62.87	62.25	61.74	57.94	57.07	57.83	13.48	13.26	13.44
8	40 (0)	50 (0)	150 (0)	53.51	53.51	53.51	50.47	50.47	50.78	12.56	12.56	12.63
9	40 (0)	50 (0)	150 (0)	53.51	53.51	53.51	50.47	50.47	50.78	12.56	12.56	12.63
10	30 (−1)	50 (0)	200 (1)	64.49	63.30	64.73	57.59	56.89	57.48	16.28	16.42	16.21
11	50 (1)	50 (0)	200 (1)	61.94	62.50	61.52	57.83	59.08	58.29	17.29	17.63	17.47
12	50 (1)	50 (0)	100 (−1)	55.64	56.83	55.24	54.75	55.45	54.86	11.18	11.05	11.12
13	30 (−1)	50 (0)	100 (−1)	54.81	54.25	54.92	52.62	51.37	53.16	12.34	12.01	12.18
14	50 (1)	60 (1)	150 (0)	56.78	55.65	54.78	49.29	48.21	49.38	13.26	13.28	13.25
15	40 (0)	40 (−1)	200 (1)	62.63	62.69	62.74	57.19	56.80	57.37	16.18	16.06	16.13
16	40 (0)	50 (0)	150 (0)	53.51	53.51	53.51	50.47	50.47	50.78	12.56	12.56	12.63
17	40 (0)	40 (−1)	100 (−1)	57.42	56.85	57.83	50.75	50.92	50.47	10.26	10.61	10.42

X_1 – osmotic temperature (C); X_2 – osmotic solution concentration (°brix); X_3 – agitation speed (RPM); Y_{EXP} – experimental value; Y_{RSM} – predicted by RSM model; Y_{ANN} – predicted by ANN model.

tables were generated. The regression coefficients were used to make statistical calculations to generate response surface plots from the regression models.

2.5. Artificial neural network modeling

Artificial neural network can be used as an alternative to the polynomial regression based modeling tool, which provides the modeling of complex nonlinear relationships. The ANN model is potentially more accurate by including all the experimental data [29]. The reporting ability of feed-forward architecture of ANN [30,31], also known as multilayered perceptron (MLP) with back-propagation (BP) algorithm, was selected and trained in this study to develop predictive model with scaled concentrations of three variables such as osmotic temperature, osmotic solution concentration, and agitation speed as input and the water loss, weight reduction, and solid gain as output to the model, respectively. The general scheme of a multilayered perceptron neural network is shown in Fig. 1.

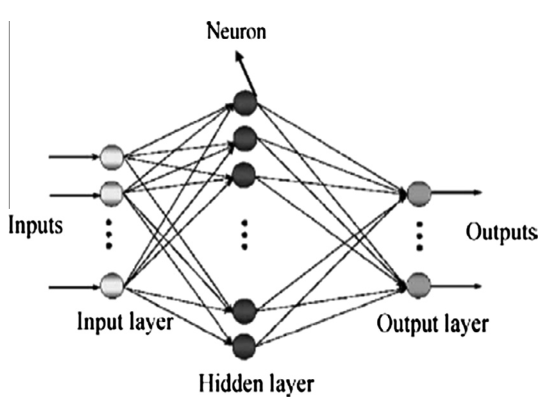

Figure 1 General scheme of a multilayered perceptron neural network.

The first step in the training of a neural network is to design the topology of the network. The number of neurons in the input layer is fixed by the number of inputs and in the output layer by the number of outputs [32]. The topology of the neural network developed was designated as 3-h-3 (three input neurons representing the three osmotic dehydration process variables, h represents hidden neurons in a single hidden layer and three output neurons representing the WL, WR, and SG). The neural network topologies were constructed, trained, tested, and validated using experimental data with a number of hidden layers varied from 3 to 10. The experimental data were divided into training, cross-validation, and testing purposes. In this study, sigmoid transfer function with back-propagation algorithm at hidden neurons and a linear transfer functions at input and output neurons were used and it is expressed as

$$f(x) = \frac{1}{1 + \exp^{(-x)}} \tag{7}$$

$$f(x) = x \tag{8}$$

The training process was run by trial and error search method until a minimum of mean square error (MSE) was reached in the validation process and the performance of trained network was estimated based on the accuracy of the neural network to produce outputs that are equal or near to target (predicted) values. In order to achieve fast convergence to the minimal root mean square error (RMSE), the inputs and outputs are scaled within the uniform range of 0 ($new\ x_{min}$) to 1 ($new\ x_{max}$) by the following equation [33] to ensure uniform attention during the training process.

$$x_{i-n} = \frac{x_i - x_{\min}}{x_{\max} - x_{\min}}(new\ x_{\max} - new\ x_{\min}) + new\ x_{\min} \tag{9}$$

where x_i is the input/output data (data of independent and dependent variable variables), x_{max} and x_{min} are the maximum and minimum values of the particular variable, respectively. MATLAB 6.5 (The Mathworks Inc.) with neural network toolbox was used for training the network model in order to generate neural network modeling and analysis.

2.6. Comparison of RSM and ANN models

In order to evaluate the goodness of fitting and prediction accuracy of the constructed models, error analyses (root mean square error (RMSE), mean absolute error (MAE), standard error of prediction (SEP), model predictive error (MPE), and chi square statistic (χ^2)) and correlation coefficients (R^2) were carried out between experimental and predicted data. The formulas used for error analyses are listed in Table 1. To study the modeling abilities of the RSM and ANN models, the values predicted by the RSM and ANN models are plotted against the corresponding experimental values.

3. Results and discussion

3.1. RSM modeling

According to the BBD, experiments were performed in order to find out the optimum combination and study the effect of process parameters on water loss, weight reduction, and solid gain for the osmotic dehydration of papaya, and the results are given in Table 2.

Linear, interactive, and quadratic models were fitted to the experimental data to obtain the regression models. Sequential model sum of squares and model summary statistics were carried out to check the adequacy of the models, and the results showed that the P-value was lower than 0.0001 for quadratic model only. Multiple regression analysis of the experimental data yielded second-order polynomial models for predicting water loss (WL), weight reduction (WR), and solid gain (SG). The second-order polynomial equation was fitted with the experimental results obtained on the basis of Box-Behnken experimental design. The final equation obtained in terms of coded factors is given below

$$\mathrm{WL} = 53.51 + 0.45X_1 + 4.19X_2 + 3.68X_3 - 7.49X_1X_2 - 0.85X_1X_3 + 0.76X_2X_3 + 0.13X_1^2 + 4.86X_2^2 + 5.58X_3^2 \tag{16}$$

$$\mathrm{WR} = 50.47 + 1.57X_1 + 4.86X_2 + 2.29X_3 - 9.30X_1X_2 - 0.47X_1X_3 - 0.66X_2X_3 - 1.21X_1^2 + 1.81X_2^2 + 6.44X_3^2 \tag{17}$$

$$\mathrm{SG} = 12.56 + 0.062X_1 - 0.045X_2 + 2.75X_3 + 0.053X_1X_2 + 0.54X_1X_3 + 0.023X_2X_3 + 0.81X_1^2 - 0.17X_2^2 + 0.9X_3^2 \tag{18}$$

The adequacy and fitness of the models were tested by Pareto analysis of variance (ANOVA), and the results indicated that the equation adequately represented the actual relationship between the independent variables and the responses (Table 3). The ANOVA result for the WL, WR, and SG shows F-value of 75.53, 74.23, and 83.87, which implies that the model is significant. Coefficient of determination (R^2) and adj-R^2 were calculated to check the adequacy and fitness of the model. The values of R^2 were calculated to be 0.9898, 0.9896, and 0.9908 for WL, WR, and SG, respectively, which implies that 95% of experimental data were compatible. The use of an adj-R^2 is to evaluate the model adequacy and fitness. The adj-R^2 value corrects the R^2 value for the sample size and for the number of terms in the model. The value of adj-R^2 (0.9767 for WL, 0.9763 for WR, and 0.979 for SG) is also high to advocate for a high significance the model.

The coefficient of variation (CV%) indicates the relative dispersion of the experimental points from the predictions of the second-order polynomial (SOP) models [39]. The value of

Table 3 ANOVA for the experimental results of the Box-Behnken design.

Source	DF	Water loss (%)			Weight reduction (%)			Solid gain (%)		
		CE	SS	P value	CE	SS	P value	CE	SS	P value
Model	9	53.51	725.61	< 0.0001	50.47	795.23	< 0.0001	12.56	68.18	< 0.0001
X_1	1	0.45	1.59	0.2614	1.57	19.69	0.0048	0.06	0.03	0.5749
X_2	1	4.19	140.37	< 0.0001	4.86	188.96	< 0.0001	−0.05	0.02	0.6846
X_3	1	3.68	108.34	< 0.0001	2.29	41.91	0.0006	2.75	60.39	< 0.0001
X_1X_2	1	−7.49	224.55	< 0.0001	−9.3	345.59	< 0.0001	0.05	0.01	0.7371
X_1X_3	1	−0.85	2.86	0.1459	−0.47	0.89	0.4151	0.54	1.18	0.0086
X_2X_3	1	0.76	2.31	0.1847	−0.66	1.72	0.2689	0.02	2.03E−03	0.8852
X_1^2	1	0.13	0.07	0.8055	−1.21	6.18	0.0568	0.81	2.79	0.0009
X_2^2	1	4.86	99.60	< 0.0001	1.81	13.81	0.0113	−0.17	0.12	0.2937
X_3^2	1	5.58	131.16	< 0.0001	6.44	174.56	< 0.0001	0.9	3.40	< 0.0001
Std. Dev.		1.03			1.09			0.3		
Mean		58.49			53.78			13.29		
CV%		1.77			2.03			2.26		
PRESS		119.55			133.31			10.12		
Adeq. Prec		33.08			35.69			31.01		
R^2		0.9898			0.9896			0.9908		
Adj R^2		0.9767			0.9763			0.979		
Pred R^2		0.8369			0.8341			0.853		

DF – degree of freedom; CE – coefficient; SS – sum of square.

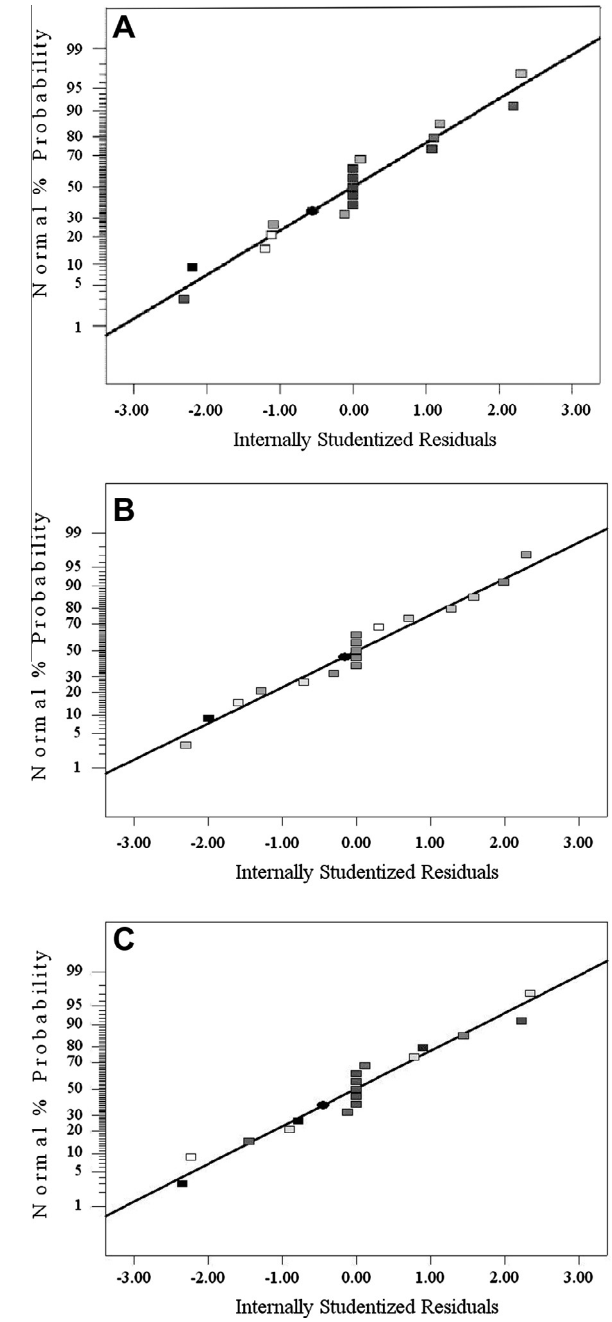

Figure 2 Normal% probability plots for WL (A), WR (B), and SG (C).

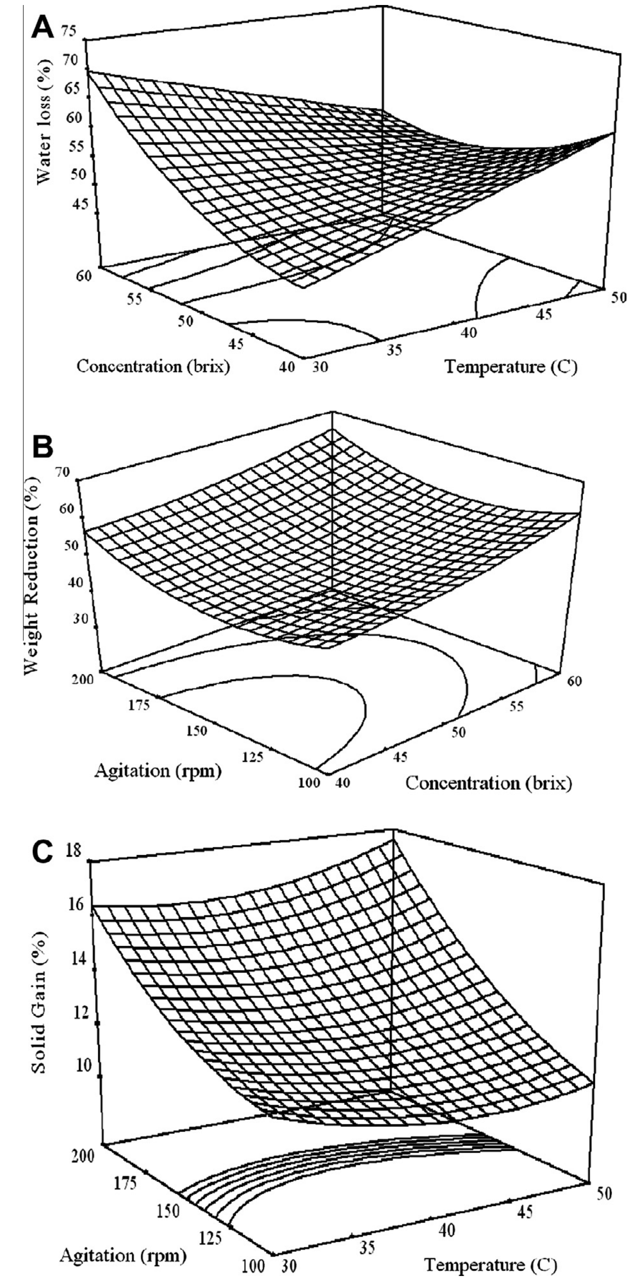

Figure 3 Response surface plot for WL (A), WR (B), and SG (C).

CV is also low as 1.77, 2.03, and 2.26, which indicates that the deviations between experimental and predicted values are low. Adequate precision measures the signal to noise ratio and this ratio is greater than 4 that is desirable [40,41]. In this work, the ratio is found to be >31, which indicates an adequate signal. Data were analyzed to check the normality of the residuals, and the normal percentage probability plot of these residuals is shown in Figs. 2A–C.

3.2. Response surface and contour plots

Response surface plots as a function of two factors at a time, maintaining all other factors at fixed levels are more helpful in understanding both the main and the interactive effects of these two factors. The response surface curves were plotted to understand the interaction of the variables and to determine the optimum level of each variable for maximum response. The response surface plots for water loss (WL), weight reduction (WR), and solid gain (SG) are shown in Fig. 3, and it shows the effects of process variables such as processing temperature, osmotic solution concentration, and agitation on water loss, weight reduction, and solid gain during the osmotic dehydration of papaya. The higher processing temperature and solution concentration promote rapid water loss (Fig. 3A) and thus reduced the time required to reach equilibrium concentrations. The rate of removal of water and solid gain is relatively high at the beginning stages, because of the high osmotic driving force between the solution concentration and the fresh sample.

Rapid removal of water in the early stages of osmotic dehydration has been reported by several authors [42–45]. During osmotic dehydration, water removal from the product is always accompanied by the simultaneous counter diffusion of solutes from the osmotic solution into the tissue. Acceleration of water loss without modification of solid gain when the dehydration solution concentration is increased [46–48]. This effect is generally attributed by the influence of natural tissue membranes as well as to the diffuse properties of water and solutes.

When water loss and solid gain take place parallel mode, the rate of water loss is always higher than the solid gain. Increase in the solid gain lowering the rates of water loss and consequently weight reduction also. Increase in the concentration and agitation leads to more water loss than solid gain which causes an increase in the weight reduction (Fig. 3B). This phenomenon is attributed to the diffusion differences between water and solutes as related to their molar masses [3,4,34,49]. The effect of high temperature yield better water transfer characteristics on the product surface due to the viscosity of the osmotic medium. Mavroudis et al. [50] affirm that the increase in agitation level could hinder the contact between the food material and the osmotic solution, causing a reduction in the mass transfer rates at a highly concentrated viscous solution. High agitation creates solution circulation and caused the intensive turbulence over the fruits pieces. The increase in the level of agitation leads to increase the water loss gradually, whereas solid gain was not affected significantly (Fig 3C).

3.3. Optimization

Optimum condition for osmotic dehydration of papaya was determined to obtain maximum water loss, weight reduction, and minimum solid gain. Second-order polynomial models obtained in this study were utilized for each response in order to obtain specified optimum conditions. In order to optimizing osmotic dehydration, the following constraints taken (1) Temperature (30–50 °C), (2) Concentration (40–60 °brix), and (3) Agitation speed (100–200 rpm). Water loss and weight reduction value must be as high as possible and solid gain value must be as low as possible. The Derringer's desirability function method was employed to optimize the process variables for covering the criteria, and the optimum conditions were found to be osmotic temperature of 32 °C, osmotic solution concentration of 60 °brix, and agitation speed 100 rpm, respectively. At this optimum conditions, water loss, weight reduction, and solid gain were found to be 68.45 (g/100 g of sample), 66.73 (g/100 g of sample), and 11.26 (g/100 g of sample) with overall desirability value of 0.906. Osmotic dehydration experiments were conducted at this optimum conditions, and determined parameters (mean of three measurements) for WL, WR, and SG were 67.28 ± 0.83 (g/100 g of sample), 65.49 ± 0.71 (g/100 g of sample), and 10.98 ± 0.59 (g/100 g of sample). The variation of 1.7%, 1.8%, and 2.5% was calculated between the predicted and experimental values. This indicates the suitability of the developed models.

3.4. ANN modeling

ANN-based process model was developed using the most popular feed-forward ANN architecture namely, multilayer perceptron (MLP) with sigmoidal function. The first step of ANN modeling was to optimize a neural network with the aim of obtaining an ANN mode with a minimal dimension and minimal errors in training and testing. The design of experiments and their respective experimental yield was used for training the network. The MLP network has three input nodes and three output nodes. The inputs chosen in this study are osmotic temperature, osmotic solution concentration, and agitation speed, while the outputs are water loss, weight reduction, and solid gain. The data portioning (training set, testing test, and cross-validation set) had been done to avoid over-training and over-parameterization. The optimal numbers of neurons in the hidden layer of the neural network are investigated by varying the number of neurons in the hidden layer and also for various combinations of ANN-specific parameters like learning rate and initialization. The generalization capac-

Table 4 Comparison between RSM and ANN.

Statistical parameters	Water loss (%)		Weight reduction (%)		Solid gain (%)	
	RSM	ANN	RSM	ANN	RSM	ANN
Error prediction						
RMSE	0.138	0.123	0.154	0.023	0.011	0.003
MAE	0.486	0.377	0.330	0.155	0.087	0.054
SEP (%)	0.375	0.334	0.455	0.070	0.139	0.044
MPE (%)	0.528	0.398	0.635	0.024	0.654	0.418
Chi square	0.131	0.115	0.163	0.024	0.047	0.015
R^2	0.989	0.992	0.989	0.999	0.990	0.997

Model summary		
Model summary	RSM	ANN
Computational time	Short	Long
Experimental domain	Regular	Irregular or regular
Understanding	Easy	Moderate
Model developing	With interactions	No interactions
Application	Frequently	Frequently

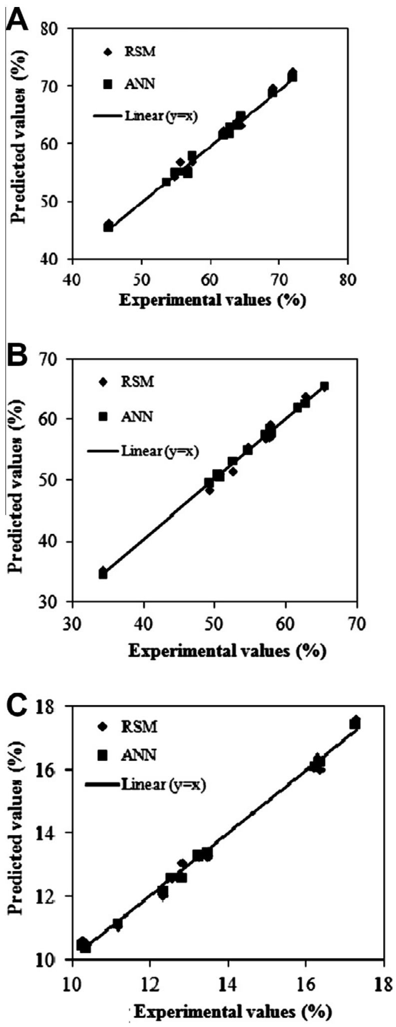

Figure 4 Comparison of experimental with predicted values of RSM and ANN models plot for WL (A), WR (B), and SG (C).

ity of the model was ensured by selecting the weights resulting in the least set RMSE between experimental and their corresponding predicted values. Each layer's initial weight and bias value was calculated to determine the structure of the trained network. The data predicted by the ANN model are given along with the RSM predicted and experimental values (Table 2).

3.5. Comparison of RSM and ANN models

Both well trained ANN and RSM models were compared with their predictive capability. The predicted values by ANN as well as the RSM models are tabulated in Table 2. An extensive statistical analysis, in terms of various statistical parameters such as RMSE, MAE, SEP (%), MPE (%), and chi square (χ^2), has been calculated by Eqs. (10–15) to compare the results. The results of the statistical analysis and comparison between RSM and ANN models are listed in Table 4.

The results showed that RSM models are larger than ANN models, indicating that the ANN model has higher modeling ability rather than the RSM models for osmotic dehydration of papaya. Linear regression analysis was carried out between the response (WL, WR, and SG) values predicted by ANN and RSM models with their corresponding experimental values and it is shown in Fig. 4.

The ANN model predictions are lie much closer to the line of perfect prediction than the RSM models. Thus, the ANN model shows a significantly higher generalization capacity than the RSM models. This higher predictive accuracy of the ANN can be attributed to its universal ability to approximate the nonlinearity of the system, whereas the RSM is restricted to a second-order polynomial. Generation of ANN model requires a large number of iterative calculations, whereas it is only a single step calculation for a response surface model. ANN model may require a high computational time to create and more costly than a response model.

4. Conclusion

This study compares the performance of RSM and ANN methodologies with their modeling, prediction, and generalization capabilities using the experimental data based on the Box-Behnken design in the osmotic dehydration process of papaya. The ANN models are found to be capable of better predictions of water loss, weight reduction, and solid gain within the range they trained than the RSM models. The results of the ANN model indicate that it is much more robust and accurate in estimating the values of dependent variables when compared with the RSM models. The structured nature of the RSM is useful to exhibit the factors contributions from the coefficients in the regression models. This ability is powerful in identifying the insignificant main factors and interaction factors or insignificant quadratic terms in the model and thereby can reduce the complexity of the problem. However, ANN has consistently performed better than the RSM in all aspects.

References

[1] S. Prakash, N. Jha datta, Performance evaluation of blanched carrots dried by three different driers, J. Food Eng. 62 (2004) 305.
[2] K.J. Park, A. Bin, F.P.R. Brod, Drying of pear d'Anjou with and without osmotic dehydration, J. Food Eng. 56 (2002) 97–103.
[3] D. Torregiani, Osmotic dehydration in fruit and vegetable processing, Food Res. Int. 26 (1993) 59–69.
[4] O. Corzo, E.R. Gomez, Optimization of osmotic dehydration of cantaloupe using desired function methodology, J. Food Eng. 64 (2004) 213–219.
[5] A.P. Sahu, A.K. Saxena, Enhanced translocation of particles from lungs by jaggery, Environ. Health. Perspect. 102 (1994) 211–214.
[6] B. Fontaniella, C. Vicente, M.E. Legaz, R.De. Armas, C.W. Rodriguez, M. Martinez, D. Pinõn, R. Acevedo, M.T. Solas, Yellow leaf syndrome modifies the composition of sugarcane juices in polysaccharides, phenols and polyamines, Plant. Physiol. Biochem. 41 (2003) 1027–1036.
[7] A.L. Raoult-Wack, Advances in osmotic dehydration, Trends. Food. Sci. Technol. 5 (1994) 255–260.
[8] N.K. Rastogi, K.S.M.S. Raghavarao, Effect of temperature and concentration of osmotic dehydration of coconut, LWT – Food, Sci. Technol. 27 (1994) 264–567.
[9] N.K. Rastogi, K.S.M.S. Raghavarao, Kinetics of osmotic dehydration of coconut, J. Food Process Eng. 18 (1995) 187–197.
[10] N.K. Rastogi, K.S.M.S. Raghavarao, Water and solute diffusion coefficients of carrot as a function of temperature and concentration, J. Food Eng. 34 (1997) 429–440.

[11] N.K. Rastogi, K.S.M.S. aghavarao, K. Niranjan, Mass transfer during osmotic dehydration of banana: Fickian diffusion in cylindrical configuration, J. Food Eng. 31 (1997) 423–432.

[12] N.K. Rastogi, K.S.M.S. Raghavarao, K. Niranjan, D. Knorr, Recent developments in osmotic dehydration: methods to enhance mass transfer, Trends. Food. Sci. Technol. 13 (2002) 58–69.

[13] J. Prakash Maran, V. Sivakumar, R. Sridhar, V. Prince Immanuel, Development of model for mechanical properties of tapioca starch based edible films, Ind. Crop. Prod. 42 (2013) 159–168.

[14] J.P. Maran, V. Sivakumar, R. Sridhar, K. Thirgananasambandham, Development of model for barrier and optical properties of tapioca starch based edible films, Carbohyd. Polym. 92 (2013) 1335–1347.

[15] J. Prakash Maran, S. Manikandan, C. Vigna Nivetha, R. Dinesh, Ultrasound assisted extraction of bioactive compounds from *Nephelium lappaceum* L. fruit peel using central composite face centered response surface design, Arab. J. Chem. (2013), http://dx.doi.org/10/1016/j.arabjc.2013.002.007.

[16] A.A. El-Aouar, P.M. Azoubel, J.L. Barbosa Jr, F.E. Xidieh Murr, Influence of the osmotic agent on the osmotic dehydration of papaya (*Carica papaya* L.), J. Food Eng. 75 (2006) 267–274.

[17] M. Ozdemir, B.F. Ozen, L.L. Dock, J.D. Floros, Optimization of osmotic dehydration of diced green peppers by response surface methodology, LWT – food, Sci. Technol. 41 (2008) 2044–2050.

[18] G.D. Mercali, L.D.F. Marczak, L.C. Tessaro, C.P. Zapata Noreña, Evaluation of water, sucrose and NaCl effective diffusivities during osmotic dehydration of banana (*Musa sapientum*, shum), LWT – Food. Sci. Technol. 44 (2011) 82–91.

[19] E. Latrille, G. Corrieu, J. Thibault, pH prediction and final fermentation time cross flow microfiltration using neural networks, Comput. Chem. Eng. 17 (1993) 423–428.

[20] M. Dornier, M. Decloux, G. Trystram, A. Lebert, Dynamic modelling of cross flow micro filtration using neural networks, J. Membrane. Sci. 98 (1995) 263–273.

[21] S. Kerdpiboon, W.L. Kerr, S. Devahastin, Neural network prediction of physical property changes of dried carrot as a function of fractal dimension and moisture content, Food. Res. Int. 39 (2006) 1110–1118.

[22] K. Movagharnejad, M. Nikzad, Modeling of tomato drying using artificial neural network, Comput. Electron. Agr. 59 (2007) 78–85.

[23] A.I. Martynenko, S.X. Yang, Biologically inspired neural computation for ginseng drying rate, Biosyst. Eng. 95 (2006) 385–396.

[24] J.A. Hernandez-Perez, M.A. Garcia-Alvarado, G. Trystram, B. Heyd, Neural networks for heat and mass transfer prediction during drying of cassava and mango, Innov. Food. Sci. Emerg. Technol. 5 (2004) 57–64.

[25] I.C. Trelea, A.L. Raoult-Wack, G. Trystram, Application of neural network modelling for the control of dewatering and impregnation soaking process (osmotic dehydration), Food Sci. Technol. Int. 3 (1997) 459–465.

[26] B.F. Ozen, L.L. Dock, M. Ozdemir, J.D. Floros, Processing factors affecting the osmotic dehydration of diced green peppers, Int. J. Food. Sci. Technol. 37 (2002) 497–502.

[27] J. Prakash Maran, S. Manikandan, K. Thirugnanasambandham, C. Vigna Nivetha, R. Dinesh, Box-Behnken design based statistical modeling for ultrasound-assisted extraction of corn silk polysaccharide, Carbohyd. Polym. 92 (2013) 604–611.

[28] J. Prakash Maran, V. Mekala, S. Manikandan, Modeling and optimization of ultrasound-assisted extraction of polysaccharide from *Cucurbita moschata*, Carbohyd. Polym. 92 (2013) 2018–2026.

[29] Y. Nagata, K.H. Chu, Optimization of a fermentation medium using neural networks and genetic algorithms, Biotechnol. Lett. 25 (2003) 1837–1842.

[30] E. Razmi-Rad, B. Ghanbarzadeh, S.M. Mousavi, Z. Emam-Djomeh, J. Khazaei, Prediction of rheological properties of Iranian bread dough from chemical composition of wheat flour by using artificial neural networks, J. Food Eng. 81 (2007) 728–734.

[31] K. Hornik, M. Stinchocombe, H. White, Multilayer feed forward networks are universal approximates, Neural Networks 2 (1989) 359–366.

[32] J. Wang, W. Wan, Optimization of fermentative hydrogen production process using genetic algorithm based on neural network and response surface methodology, Int. J. Hydrogen Energy 34 (2009) 255–261.

[33] I. Dahlan, Z. Ahmad, M. Fadly, K.T. Lee, A.H. Kamaruddin, A.R. Mohamed, Parameters optimization of rice husk ash (RHA)/CaO/CeO_2 sorbent for predicting SO_2/NO sorption capacity using response surface and neural network models, J. Hazard. Mater. 178 (2010) 249–257.

[34] R.M. García-Gimeno, C. Hervás-Martínez, R. Rodríguez-Pérez, G. Zurera-Cosano, Modeling the growth of *Leuconostoc mesenteroides* by artificial neural networks, Int. J. Food Microbiol. 105 (2005) 317–332.

[35] S. Youssefi, Z. Emam-Djomeh, S.M. Mousavi, Comparison of artificial neural network (ANN) and response surface methodology (RSM) in the prediction of quality parameters of spray-dried pomegranate juice, Dry. Technol. 27 (2009) 910–917.

[36] M. Zafar, S. Kumar, S. Kumar, A.K. Dhiman, Optimization of polyhydroxybutyrate (PHB) production by *Azohydromonas lata* MTCC 2311 by using genetic algorithm based on artificial neural network and response surface methodology, Biocatal. Agri. Biotech. 1 (2012) 70–79.

[37] A. Çelekli, F. Geyik, Artificial neural networks (ANN) approach for modeling of removal of Lanaset Red G on *Chara contraria*, Bioresour. Technol. 102 (2011) 5634–5638.

[38] M. Rajendra, P.C. Jena, H. Raheman, Prediction of optimized pretreatment process parameters for biodiesel production using ANN and GA, Fuel 88 (2009) 868–875.

[39] J. Prakash Maran, V. Sivakumar, K. Thirgananasambandham, R. Sridhar, Model development and process optimization for solvent extraction of polyphenols from red grapes using Box-Behnken design, Prep. Biochem. Biotech. (2013), http://dx.doi.org/10(1080/10826068), 2013, 791629.

[40] J. Prakash Maran, S. Manikandan, Response surface modeling and optimization of process parameters for aqueous extraction of pigments from prickly pear (*Opuntia ficus-indica*) fruit, Dye. Pigm. 95 (2012) 465–472.

[41] J. Prakash Maran, S. Manikandan, B. Priya, P. Gurumoorthi, Box-Behnken design based multi-response analysis and optimization of supercritical carbon dioxide extraction of bioactive flavonoid compounds from tea (*Camellia sinensis* L.) leaves, J. Food Sci. Technol. (2013), doi: http://dx.doi.org/10.1007/s13197-013-0985-z.

[42] F.K. Ertekin, T. Akaloz, Osmotic dehydration of peas: I. Influence of process variables on mass transfer, J. Food. Process. Preserv. 20 (1996) 87–104.

[43] P. Genina-Soto, J. Barrera-Cortes, G. Gutierra-Lopez, A.E. Nieto, Temperature and concentration effects of osmotic media on osmotic dehydration profiles of sweet potato cubes, Dry. Technol. 19 (2001) 547–558.

[44] H.N. Lazarides, E. Katsanidis, A. Nickolaidis, Mass transfer kinetics during osmotic preconcentration aiming at minimal solid uptake, J. Food Eng. 25 (1995) 151–166.

[45] J. Shi, M. Le Maguer, Osmotic dehydration of foods: mass transfer and modeling aspects, Food. Rev. Int. 18 (2002) 305–335.

[46] D.R. Bongirwar, A. Sreenivasan, Studies on osmotic dehydration of bananas, J. Food. Sci. Technol. 14 (1977) 104–112.

[47] J. Hawkes, J.M. Flink, Osmotic concentration of fruit slices prior to freeze dehydration, J. Food. Process. Preserv. 2 (1978) 265–284.
[48] M.N. Islam, J.M. Flink, Dehydration of potato. II. Osmotic concentration and its effect on air drying behaviour, J. Food Technol. 17 (1982) 387–403.
[49] A.L. Raoult-Wack, S. Guilbert, M. Le Maguer, G. Andrios, Simultaneous water and solute transport in shrinking media: application to dewatering and impregnation soaking process analysis (osmotic dehydration), Dry. Technol. 9 (1991) 589–612.
[50] N.E. Mavroudis, V. Gekas, I. Sjoholm, Osmotic dehydration of apples – effect of agitation and raw material characteristics, J. Food Eng. 35 (1998) 191–209.